

SHR-A1811, a novel anti-HER2 antibody–drug conjugate with optimal drug-to-antibody ratio, superior bystander killing effect and favorable safety profiles

Ting Zhang

Shanghai Hengrui Pharmaceutical Co., Ltd.

Jiayan Xu

Shanghai Hengrui Pharmaceutical Co., Ltd.

Junzhao Yin

Shanghai Hengrui Pharmaceutical Co., Ltd.

Yun Gao

Shanghai Hengrui Pharmaceutical Co., Ltd.

Hanwen Zheng

Shanghai Hengrui Pharmaceutical Co., Ltd.

Beibei Fu

Shanghai Hengrui Pharmaceutical Co., Ltd.

Jiakang Sun

Shanghai Hengrui Pharmaceutical Co., Ltd.

Zhibing Xu

Shanghai Hengrui Pharmaceutical Co., Ltd.

Shiwei Tu

Shanghai Hengrui Pharmaceutical Co., Ltd.

Yuchang Mao

Shanghai Hengrui Pharmaceutical Co., Ltd.

Weiyun Wen

Shanghai Hengrui Pharmaceutical Co., Ltd.

Bolei Qu

Shanghai Hengrui Pharmaceutical Co., Ltd.

Lingfeng You

Shanghai Hengrui Pharmaceutical Co., Ltd.

Zhendong Xue

Shanghai Hengrui Pharmaceutical Co., Ltd.

Xing Sun

Shanghai Shengdi Pharmaceutical Co. Ltd.

Dan Cao

Shanghai Hengrui Pharmaceutical Co., Ltd.

Jun Feng

Shanghai Hengrui Pharmaceutical Co., Ltd.

Min Hu

min.hu@hengrui.com

Shanghai Hengrui Pharmaceutical Co., Ltd.

Feng He



Shanghai Hengrui Pharmaceutical Co., Ltd.

Research Article

Keywords: anti-HER2 ADC, permeability, drug-to-antibody ratio, bystander killing effect, safety profile

Posted Date: December 29th, 2023

DOI: <https://doi.org/10.21203/rs.3.rs-3770094/v1>

License:   This work is licensed under a Creative Commons Attribution 4.0 International License. [Read Full License](#)

Additional Declarations: No competing interests reported.

Abstract

Background

HER2-targeting antibody–drug conjugates (ADCs), especially trastuzumab deruxtecan (T-DXd), have revolutionized the treatment landscape of HER2-expressing or mutant cancers. However, undesired adverse events are still inevitable. It is necessary to discover a novel HER2-directed ADC with better safety profiles.

Methods

SHR-A1811 is composed of trastuzumab, a cleavable linker and a novel topoisomerase I inhibitor, SHR169265. The permeability and pharmacokinetics of SHR169265 were detected by PAMPA assay and LC-MS/MS System. CellTiter-Glo cell viability assay was used to determine the cytotoxicity and bystander killing effect of SHR169265 and SHR-A1811. The antitumor efficacy of SHR-A1811 was evaluated in mouse xenograft models with different HER2 expression levels. The toxicity of SHR-A1811 were evaluated in cynomolgus monkeys.

Results

SHR169265 showed better permeability, stronger cytotoxicity and faster systemic clearance than SHR197971 (a DXd analog). The drug-to-antibody ratio (DAR) of SHR-A1811 was optimized as 6 via balancing efficacy and toxicity. SHR-A1811 showed HER2-dependent growth inhibition against various cell lines and desirable bystander killing capability. SHR-A1811 led to tumor growth inhibition or even regression in a dose-dependent manner, at least comparable as HRA18-C015 (a biosimilar of T-DXd) and anti-HER2-SHR169265 (DAR 8) in multiple xenograft models with a range of HER2 expression levels. SHR-A1811 exhibited a good pharmacokinetics profile, outstanding stability in plasma across different species and a favorable preclinical safety profile. The highest non-severely toxic dose (HNSTD) in cynomolgus monkeys was 40 mg/kg with thymus as the main target organ.

Conclusions

SHR-A1811 is a potential best-in-class anti-HER2 ADC with a highly permeable payload, optimized DAR, great potency and better safety profiles. Currently SHR-A1811 has entered phase II and phase III clinical studies for breast cancer, gastric cancer, colorectal cancer, and NSCLC.

Introduction

Human epidermal growth factor receptor 2 (ERBB2, HER2) is a well-validated proto-oncogene, overexpressed, amplified or mutated in multiple advanced solid tumors [1–3]. Trastuzumab deruxtecan (T-DXd, DS-8201a, ENHERTU), a representative of the third-generation ADC, has been approved for the treatment of HER2-expressing breast cancer, gastric cancer and HER2 mutant non-small cell lung cancer (NSCLC) [4–7]. It is structurally composed of HER2 antibody trastuzumab, a cleavable peptide-based linker and a topoisomerase I inhibitor payload MAAA-1181a (DXd, exatecan derivative) [8, 9]. The high drug load (DAR 8) and bystander killing effect made T-DXd the first HER2-targeted therapy showing clinical benefit in HER2 low-expressing (IHC 1 + or IHC 2+/FISH-) breast cancer [5, 8–10]. However, although a stable linker and high systemic clearance of payload were designed to minimize toxicities, the high rate of associated adverse effects, such as hematologic and gastrointestinal disorders, left ventricular dysfunction and interstitial lung disease (ILD)/pneumonitis, pointed to a room for further improvement [11, 12].

T-DXd has been issued a black box warning for the risk of ILD/ pneumonitis [13]. Permanent treatment cessation is recommended with grade 2 or higher ILD/pneumonitis [14]. The pooled clinical data analysis (DS8201-A-J101, DESTINY-Breast01, DESTINY-Breast03, DESTINY-Breast04, and DESTINY-Lung02) suggested that the incidence of ILD/pneumonitis was 12% in patients treated with 5.4 mg/kg of T-DXd [5, 14–17]. In the global phase III study in HER2-positive metastatic breast cancer patients (DESTINY-Breast03), where patients received 5.4 mg/kg of T-DXd, treatment discontinuation occurred in 14% of patients and ILD/pneumonitis accounted for 8%. Moreover, the dose interruption and reduction rates in T-DXd arm were 44% and 21%, respectively, mainly due to neutropenia, leukopenia and nausea, etc. The incidence of drug-related adverse events of grade 3 or 4 reached 45.1% [18]. In DESTINY-Gastric01 trial, 15% of discontinuation rate was observed in patients receiving 6.4 mg/kg of T-DXd, and ILD/pneumonitis accounted for 6%. Dose

interruption occurred in up to 62% of patients [6]. Therefore, it is necessary to discover a novel anti-HER2 ADC with better safety margin, without jeopardizing the efficacy.

In this study, we described SHR-A1811, a HER2-ADC consisted of trastuzumab, a cleavable linker and a unique topoisomerase I inhibitor payload SHR169265. SHR169265 was designed to increase the permeability and bystander killing effect. The DAR value of SHR-A1811 was optimized as 6. The enhanced bystander killing effect ensured a comparable antitumor efficacy of SHR-A1811 as T-DXd, even though with lower DAR. The chemical modification of SHR169265 also improved the stability of SHR-A1811. Optimized DAR and high stability together led to desirable safety profiles in GLP toxicity study in cynomolgus monkeys. Collectively, these favorable preclinical profiles supported SHR-A1811 a potential best-in-class HER2-targeting ADC, and multiple clinical trials are ongoing in patients with HER2-expressing and/or mutant cancers.

Materials and Methods

Antibody–drug conjugates and chemicals

SHR167971 were synthesized using published DXd structure [8]. Trastuzumab was produced with the published amino acid sequence [19]. HRA18-C015 and HRA18-K001 were synthesized according to the published T-DXd and TDM-1 structure [8, 20]. Anti-HER2-SHR169265 (DAR 4), SHR-A1811, and anti-HER2-SHR169265 (DAR 8) were composed of trastuzumab, a maleimide glycyl-glycyl-phenylalanyl-glycyl (GGFG) peptide linker and SHR169265 with the DAR values at 4, 6 and 8, respectively. Human IgG1-ADC was composed of isotype control IgG1, GGFG linker and SHR169265 with DAR at 8. The four inter-strand disulfide bonds of antibodies were reduced to eight cysteine residues by tris(2-carboxyethyl) phosphine. The linker and payload were connected as described previously [21]. Linker-payload was conjugated to the cysteine residues using a conventional strategy [22].

Distribution coefficient (Log D, pH 7.4)

Distribution coefficient (Log D, pH 7.4) was obtained by a high-throughput alternative method [23]. Each compound was dissolved in DMSO at 10 mM. After centrifugation, the solution was measured by reversed-phase HPLC on a C18 column (50×4.6 mm, 5 μM Gemini C18, Phenomenex) at pH 7.4, using fast gradient acetonitrile-aqueous buffer mobile phases. The lipophilicity was estimated from a calibration curve using six reference compounds by plotting their respectively measured retention time versus LogD in literature. The chromatographic LogD values were derived directly from the gradient retention time by using this calibration curve.

Parallel artificial membrane permeability (PAMPA) assay

PAMPA assay was outsourced to Wuxi Apptech Co. Ltd. Briefly, donor plate, acceptor plate and receiver plate formed a sandwich. 200 μL of 5.0 μM donor solutions were added. The concentrations of compounds in both plates were measured by a LC-MS/MS system after 30 minutes. The permeability coefficient (P_{eff}, nm/s) values at pH 5 and 7.4 were calculated.

Topoisomerase I inhibition assay

Topoisomerase I inhibition assay was outsourced to Wuxi Apptech Co. Ltd. Topoisomerase I activity was measured using human topoisomerase I microplate assay kit (Inspiralis), according to the manufacturer's instructions.

Pharmacokinetics of payload in mice

All animal experiments at Shanghai Hengrui were approved by Shanghai Hengrui's Institutional Animal Care and Use Committee. Studies were performed in accordance with ARRIVE guidelines. C57BL/6 mice (15–18 g body weight) were purchased from Beijing Vital River Laboratory Animal Technology Co., Ltd. Compounds were administered intravenously at 0.5 mg/kg. Blood samples were collected at various time points after dosing. The compound concentrations were determined by SCIEX Triple Quad 7500 LC-MS/MS System (SCIEX).

Cell lines

The human breast cancer cell lines SK-BR-3, HCC1954 and MDA-MB-468, the human gastric carcinoma cell lines NCI-N87, AGS and ANU-16, and the human pancreatic cancer cell line Capan-1 were purchased from American Type Culture Collection. The human breast cancer cell line JIMT-1 was purchased from Cobioer Biosciences Co. LTD. The human gastric carcinoma cell line MKN-45 was purchased from Japanese Collection of Research Bioresources Cell Bank. MDA-MB-468 cell line was cultured in Leibovitz's L-15 medium (Gibco) supplemented with 10% FBS (Gibco) at 37°C without CO₂. All other cell lines were cultured with appropriate medium

(DMEM (Gibco) for JIMT-1; RPMI1640 (Gibco) for HCC1954, NCI-N87, AGS, SNU-16 and MKN-45; McCoy's 5A (Gibco) for SK-BR-3; and IMDM (Gibco) for Capan-1) supplemented with 10% FBS at 37°C under 5% CO₂ atmosphere.

Flow cytometry analysis of HER2 expression

2×10⁵ cells were incubated with BB700 mouse anti-human HER2 antibody (BD Biosciences) at 1µg/mL for 30 minutes at 4°C. The fluorescent signal was detected using BD FACSVerse. The data was analyzed by FlowJo_v10.8.1 (BD Biosciences).

Cell viability assay

Cells were seeded into 96-well plates at 1500 cells/well for SK-BR-3, JIMT-1 and NCI-N87, 800 cells/well for HCC1954, 600 cells/well for AGS and MKN-45, 2500 cells/well for MDA-MB-468 and Capan-1, and 1000 cells/well for SNU-16. After overnight incubation, a serially diluted solution of compounds or ADCs was added. Cell viability was evaluated after 6 days using CellTiter-Glo reagent (Promega) according to the manufacturer's instructions. Luminescence was measured by PHERAstar (BMG LABTECH).

Western blot analysis

SK-BR-3 cells were incubated with 2 nM of ADCs for 48 hours and then lysed in lysis buffer (Cell Signaling Technology) containing PMSF and PhosSTOP (Roche). 20–60 µg of protein lysates were separated by SDS-PAGE gel and electro-transferred to polyvinylidene difluoride membranes. Blots were probed by anti-cleaved PARP (Asp214) antibody, anti-phospho-Histone H2A.X (Ser139) antibody, anti-GAPDH (D16H11) XP Rabbit antibody and anti-HSP70 antibody (Cell Signaling Technology) at appropriate concentrations. The membranes were subsequently incubated with secondary antibody (anti-rabbit IgG, Cell Signaling Technology) and Supersignal kit (Thermo Scientific). The chemiluminescence signal was detected using a ChemiDoc MP imaging System (Bio-Rad).

Caspase-Glo 3/7 assay

SK-BR-3 cells were treated with a serially diluted solution of ADCs for 3 days. The Caspase-Glo™ 3/7 reagent (Promega) was added according to manufacturer's guidelines. Luminescence was measured by PHERAstar (BMG LABTECH).

Bystander killing effect

HER2-positive SK-BR-3 and HER2-negative MDA-MB-468 cells were seeded together into 6-well plates at 1.5×10⁵ cells/well and 1×10⁵ cells/well, respectively. Cells were treated with ADCs for 3 or 5 days. In order to determine the ratio of SK-BR-3 and MDA-MB-468 in each well, cells were harvested at endpoint to count total number and stained with BB700 mouse anti-human HER2 antibody (BD Biosciences). The fluorescent signal of stained cells was analysed using BD FACSVerse. Based on the ratio of positive vs. negative cells, the residual numbers of SK-BR-3 and MDA-MB-468 cells in each well were calculated.

Mouse xenograft experiments

Female NUNU nude mice, Beige scid mice and Balb/c nude mice (15–18 g body weight) were purchased from Beijing Vital River Laboratory Animal Technology Co., Ltd. In brief, NCI-N87 (5×10⁶ cells/inoculation), JIMT-1 (4.5×10⁶ cells/inoculation) and Capan-1 (3×10⁶ cells/inoculation) were implanted subcutaneously into the hind flank region and allowed to grow to the appropriate size (150–250 mm³ in average). Six to eight mice per treatment group were randomized according to the size of tumors. The ADCs were administered intraperitoneally at various dosages single time or every week for two weeks. Tumor volume and body weight were measured twice a week during the course of the study. Tumor growth inhibition (TGI, %) was calculated as $TGI\% = [1 - (T - T_0) / (C - C_0)] \times 100\%$, where C₀ and T₀ stand for the average tumor volume of vehicle and treatment groups at study start, and C and T for the average tumor volume of vehicle and treatment groups at endpoint. Tumor volume of individual tumors at each time point was measured as $V = 1/2 \times \text{Length} \times \text{Width}^2$.

Immunohistochemistry

NCI-N87, JIMT-1 and Capan-1 xenografted tumors were harvested and fixed in 10% neutral buffered formalin and embedded in paraffin. For antigen retrieval, the sections were incubated at 100°C for 15 minutes in EDTA buffer (pH 9.0). After blocking of nonspecific reactions by 1.5% BSA, the sections were incubated with anti-Her2/neu antibody (clone SP3; 1:100; Invitrogen) for 60 minutes at room temperature. The sections were then washed and incubated with polymer-based signal amplification system (ImmPRESS® HRP Horse Anti-Rabbit IgG Polymer Detection Kit, Vector Laboratories) for 30 minutes. The 0.01% diaminobenzidine (DAB, MaiXin Biotech) was used to develop a brown chromogen, and the mounted slides were scanned.

PK/PD study

In the NCI-N87 xenograft model, blood samples and tumor tissues were collected at 8, 24, 72 and 168 hours after single dose of ADCs. The cleaved PARP level in tumors were detected using western blotting. The concentrations of payload in tumor and blood samples were detected by SCIEX Triple Quad 7500 LC-MS/MS System (SCIEX).

Pharmacokinetics in rats

SD rats (160–180 g body weight) were purchased from Beijing Vital River Laboratory Animal Technology Co., Ltd. After an adaptation period, rats were randomly divided into three groups (n = 4 for each group). 3 mg/kg of SHR-A1811 was intravenously administered. Blood sample was collected at various time points after dosing. The concentration of total antibody and intact ADC were determined by HTRF method.

In vitro stability of SHR-A1811 in plasma

20 µg/mL of SHR-A1811 was incubated in mouse, rat, monkey, and human plasma at 37°C for up to 21 days. The concentrations of released payload were quantified by SCIEX Triple Quad 7500 LC-MS/MS System (SCIEX). The released payload proportional to the theoretical concentration of all payload in ADC was calculated as: release rate (%) = $C_{\text{payload}} / (C_{\text{ADC}} \times \text{DAR}) \times 100\%$, where C stands for concentration (nM).

GLP toxicology and toxicokinetics studies in cynomolgus monkeys

GLP toxicology and toxicokinetics studies were outsourced to Shanghai InnoStar Bio-tech Co., Ltd. Studies were approved by InnoStar's Institutional Animal Care and Use Committee and carried out in compliance with ARRIVE guidelines. Briefly, SHR-A1811 was intravenously administered every 3 weeks for a total of 5 doses in cynomolgus monkeys (N = 10 for each group, 5 animals per sex). Clinical signs, body weight, food consumption, and clinical pathology were monitored. The blood samples were collected after the first and fourth doses of 40 mg/kg to measure the concentrations of SHR-A1811, total antibody and free payload.

Statistics analysis

Data are presented as means ± SEM from at least three independent experiments. GraphPad Prism software version 9 (GraphPad Software) was used for curve fitting. Differences between two groups were analyzed by a standard Student t-test. For multigroup comparisons, two-way anova were performed. P < 0.05 was considered statistically significant.

Data Availability

The data generated in this study are available upon request from the corresponding authors.

Results

Physicochemical characteristics, topoisomerase I inhibition and pharmacokinetic profile of SHR169265

SHR169265 (Fig. 1A) is an exatecan derivative with a chiral cyclopropyl at the carbonyl alpha position [21, 24], selected based on parameters including potency, solubility, permeability, and pharmacokinetics, etc. The liposolubility and permeability of SHR169265 were evaluated by LogD (pH 7.4), ALogP and Peff values. The LogD (pH 7.4) and ALogP values showed that SHR169265 had moderate liposolubility. The Peff values at pH 5 and pH 7.4 of SHR169265 were 137.7 and 71.6 nm/s, respectively, about 5 times higher than those of SHR167971 (Table 1), indicating that SHR169265 had higher membrane permeability. The inhibition of SHR169265 on DNA topoisomerase I enzymatic activity was comparable with that of SHR167971. In addition, SHR169265 showed faster systemic clearance in mice than SHR167971 (CL: 72.6 vs. 50 mL/min/kg; 0.5 mg/kg, i.v.).

Table 1
Physicochemical parameters, topoisomerase I inhibitory activity and pharmacokinetic parameters of SHR169265

		SHR169265	SHR167971
Molecule weight		533.55	493.49
Log D (pH 7.4)		1.89	1.43
AlogP (calc.)		3.67	2.72
PAMPA	pH 5	137.7	25.9
Peff (nm/s)	pH 7.4	71.6	17.5
Top I inhibition (IC ₅₀ , μM)		1.34	0.97
PK parameters in mice (0.5 mg/kg, i.v. injection)	Cmax (ng/mL)	250	343
	AUC _{0-t} (ng/mL*h)	113	154
	t1/2(h)	0.37	0.27
	CL(mL/min/kg)	72.6	54
	Vss (mL/kg)	1815	1276
SHR167971: payload synthesized with published DXd structure.			

Cytotoxicity of SHR169265

The cytotoxicity of SHR169265 was evaluated in nine cancer cell lines. Overall SHR169265 inhibited cell growth with the IC₅₀ values 2–3 times more potent than SHR167971 (Table 2). Considering their comparable inhibitory effect on topoisomerase I, the stronger cytotoxicity of SHR169265 could be attributed to its higher membrane permeability.

Table 2
Cytotoxicity of SHR169265 and anti-HER2-SHR169265 ADCs

IC ₅₀ (nM)	HER2 level	SHR169265	SHR167971	Anti-HER2-SHR169265 (DAR 4)	SHR-A1811 (DAR 6)	Anti-HER2-SHR169265 (DAR 8)	HRA18-C015 (DAR 8)	Control IgG1-ADC (DAR 8)	Trastuzumab
NCI-N87	High	1.00 ± 0.07	2.91 ± 0.53	0.85 ± 0.19	0.57 ± 0.15	0.37 ± 0.11	0.30 ± 0.04	> 100	> 100
SK-BR-3	High	0.58 ± 0.10	1.38 ± 0.23	0.66 ± 0.13	0.42 ± 0.10	0.28 ± 0.09	0.29 ± 0.15	> 10	> 3
HCC1954	High	0.55 ± 0.19	1.07 ± 0.35	1.28 ± 0.15	0.77 ± 0.10	0.44 ± 0.17	0.50 ± 0.09	> 100	> 500
JIMT-1	Medium	2.32 ± 0.45	7.85 ± 2.96	495.4 ± 65.5	302.9 ± 87	260.2 ± 12	203.8 ± 8.6	1230 ± 181.7	> 5000
Capan-1	Low	0.38 ± 0.07	1.29 ± 0.41	38.4 ± 7.7	11.3 ± 2.7	5.4 ± 1.7	11.2 ± 0.9	57.2 ± 10.3	> 500
AGS	Low	0.36 ± 0.11	0.60 ± 0.27	107.8 ± 24.5	59.1 ± 17.2	47.3 ± 8.1	30.3 ± 8.4	68.4 ± 25.1	> 500
MKN45	Low	0.30 ± 0.07	1.18 ± 0.22	82.5 ± 14.1	42.5 ± 7.8	38.5 ± 6.6	35.9 ± 6.8	74.5 ± 24.2	> 500
SNU-16	Low	0.57 ± 0.19	1.58 ± 0.25	161.8 ± 5.8	132.6 ± 22.3	88.8 ± 16.2	74.8 ± 18.6	168.3 ± 27.3	> 500
MDA-MB-468	Negative	0.56 ± 0.09	1.13 ± 0.14	146.6 ± 30.5	97.3 ± 23.1	86.8 ± 16.7	59.1 ± 12.5	206.9 ± 44.6	> 500
HRA18-C015: T-DXd biosimilar synthesized according to the published structure.									

Cell killing activity of anti-HER2-SHR169265 ADCs

Three anti-HER2-SHR169265 ADCs composed of trastuzumab, a cleavable linker and payload SHR169265 with DAR values at 4, 6, and 8 were synthesized. The linker was a maleimide glycynglycyn-phenylalanyl-glycyn (GGFG) peptide linker and can be cleaved by the enzymes in lysosome. After endocytosis, the ADCs are cleaved at the indicated position, and the first intermediate undergoes self-degradation to release the payload SHR169265 (Fig. 1A).

Nine breast cancer and gastric cancer cell lines were divided into 4 groups, HER2-high (NCI-N87, SK-BR-3, and HCC1954), HER2-medium (JIMT-1), HER2-low (capan-1, AGS, MKN45, and SNU-16) and HER2-negative group (MDA-MB-468), according to the flow cytometry analysis (Supplementary Fig. S1). Anti-HER2-SHR169265 ADCs impaired HER2-expressing cell viability without obvious effect on HER2-negative cells (MDA-MB-468). This inhibitory capacity was in general correlated with DAR value (Table 2). It was also correlated with HER2 expression levels, except that JIMT-1 cell line was an outlier, probably due to its relative insensitivity to SHR169265 (Table 2). SHR-A1811 (DAR 6) showed slightly weaker potency (1.2–1.5 fold less) than anti-HER2-SHR169265 (DAR 8) and HRA18-C015 (DAR 8), attributable to lower DAR. This seemingly inconsistency with the results of direct killing by payloads, where SHR169265 is 2–3 times more potent than SHR167971 across the cell panel, may be explained by the different routes of payload vs. ADCs to enter cells. ADCs are internalized through antibody-antigen interaction, thus their cellular activities will be less influenced by the membrane permeability of payloads, whereas more by the DAR and inhibitory activity on topoisomerase I.

To confirm the mechanism of cytotoxicity was due to inhibition of DNA topoisomerase I, the DNA damage markers (histone H2A.X phosphorylation) and apoptosis markers (cleaved PARP and caspase 3/7 levels) were analyzed on SK-BR-3 cells. All three anti-HER2-SHR169265 ADCs and HRA18-C015 significantly increased these markers (Supplementary Fig. S2). The degree of caspase 3/7 induction was correlated with DAR values.

Bystander killing effect of anti-HER2-SHR169265 ADCs

To evaluate the bystander killing effect of ADCs, HER2-positive cells (SK-BR-3) and HER2-negative cells (MDA-MB-468) were co-cultured. As expected, HRA18-K001 (a biosimilar of T-DM1) mainly inhibited HER2-positive cell growth, suggesting a poor bystander killing capacity as reported [10]. In contrast, three anti-HER2-SHR169265 ADCs and HRA18-C015 killed both HER2-positive cells and their adjacent negative cells at 10 nM (Fig. 1B), without much effect on HER2-negative cells when cultured alone. The bystander killing IC_{50} s on MDA-MB-468 cells were further analyzed in the co-culture system (Fig. 1C). Among all tested ADCs, anti-HER2-SHR169265 (DAR 8) exhibited the strongest bystander killing effect (IC_{50} , 0.17 ± 0.04 nM). SHR-A1811 (DAR 6) and HRA18-C015 (DAR 8) showed a comparable bystander killing effect (IC_{50} , 0.23 ± 0.05 vs. 0.25 ± 0.01 nM), embodying the advantage of high membrane permeability of payload.

Antitumor efficacy of anti-HER2-SHR169265 ADCs and DAR optimization

In order to determine the optimal DAR value, the antitumor efficacy of three anti-HER2-SHR169265 ADCs was evaluated in HER2-moderate JIMT-1 xenograft models (Fig. 2A) after single dose. At the dosage of 5 mg/kg, SHR-A1811 (DAR 6) led to 57.9% TGI, comparable with HRA18-C015 (59.8% TGI) and anti-HER2-SHR169265 (DAR 8) (59.4% TGI), and stronger than anti-HER2-SHR169265 (DAR 4) (46.7% TGI). The difference between SHR-A1811 and anti-HER2-SHR169265 (DAR 4) was further amplified at 10 mg/kg (TGI 80.7% vs. 57.9%) (Fig. 2B). Considering the overall *in vitro* and *in vivo* profiles, SHR-A1811 and anti-HER2-SHR169265 (DAR 8) were chosen for further evaluation to fine tune the DAR.

Three xenograft models (NCI-N87, JIMT-1 and Capan-1) with a range of HER2 expression levels were established (Fig. 2A). SHR-A1811 inhibited tumor growth in a dose-dependent manner in all three models (Fig. 2C-E), without effect on mouse body weight (Supplementary Fig. S3). In NCI-N87 (HER2-high) and Capan-1 (HER2-low) models, the TGIs of SHR-A1811, HRA18-C015 and anti-HER2-SHR169265 (DAR 8) were comparable at the same dosage. Tumor regression was observed at 3 mg/kg of SHR-A1811 and sustained till day 17 (120% TGI in NCI-N87 model; 115% TGI in Capan-1 model). Trastuzumab at 6 mg/kg caused 51% of TGI in NCI-N87 model. Control IgG1-ADC showed no effect on tumor growth. In JIMT-1 (HER2-moderate) model, the TGIs of SHR-A1811 and anti-HER2-SHR169265 (DAR 8) were greater than that of HRA18-C015 at 3 and 6 mg/kg after two doses. In this model, multiple dosing could better embody the advantages of SHR-A1811 and anti-HER2-SHR169265 (DAR 8), comparing to the results of single dose (Fig. 2B). All these data demonstrated that SHR-A1811, though with 25% less payload, conferred at least comparable antitumor activity as HRA18-C015. The enhanced membrane permeability of payload could bring in a stronger bystander effect in solid tumors, and compensate for the lower DAR used in SHR-A1811. Therefore, we finally chose SHR-A1811 (DAR 6) as our lead molecule.

PD biomarkers and released payload in plasma and NCI-N87 tumors were analyzed after single dose of SHR-A1811 or HRA18-C015. As shown in Fig. 2F, free payload was detected in tumors and the concentrations were proportional to the dosages of ADCs. At 3 and 6 mg/kg, the tumoral SHR169265 levels reached C_{max} at 24 and 72 hours after treatment, respectively. The tumoral AUC of SHR169265 and SHR-167971 were comparable at the same dosage. Consistent with the stability of ADCs and fast clearance of free payload in circulation, the levels of payloads in plasma were below the limitation of quantitation (0.1 ng/mL). In addition, SHR-A1811 treatment induced PARP cleavage in tumor cells. The degree of PD marker changes was correlated with tumoral SHR169265 levels (Fig. 2G).

Pharmacokinetics profile and plasma stability of SHR-A1811

After single intravenous injection of SHR-A1811 at 3 mg/kg in rats, the exposure levels of ADC and total antibody were measured. The PK profiles of SHR-A1811 and total antibody were similar ($T_{1/2}$; 8.3 and 8.7 days, AUC; 5598 and 6156 $\mu\text{g}\cdot\text{h}/\text{mL}$, Clearance; 11.8 and 10.6 mL/day/kg, respectively, Fig. 3A), suggesting the stability of the linker-payload system.

The release rate of SHR169265 from SHR-A1811 ranged from 0.27–0.76% after 21-day incubation in mouse, rat, monkey and human plasma (Fig. 3B), indicating an excellent *in vitro* plasma stability.

Safety profiles and toxicokinetics of SHR-A1811

The safety of multiple administration (every 3 weeks for 5 doses) of SHR-A1811 was evaluated in cynomolgus monkeys. SHR-A1811 reduced reticulocyte number and percentage by 80%, thymus weight and organ coefficient by 71% at 40 mg/kg. All adverse effects recovered after 4 weeks of drug withdrawal. No abnormalities were observed at 3 or 10 mg/kg. Therefore, the HNSTD of SHR-A1811 in cynomolgus monkeys was determined as 40 mg/kg with thymus as the main target organ (Table 3). The serum concentrations of SHR-A1811, total antibody and payload were measured after the first and fourth doses of 40 mg/kg (Fig. 4 and Table 4). The toxicokinetics parameters of SHR-A1811 after single and multiple doses were comparable, suggesting low immunogenicity. The TK profile of SHR-

A1811 was similar with that of total antibody after multiple does (T1/2: 7.1 and 7.5 days; AUC_t: 3988 and 5452 day*μg /mL, respectively). Only very small amount of free toxin was detected in plasma. The C_{max} of SHR-A1811 and payload after multiple doses were 801.1 μg/mL and 1.48 ng/mL, respectively. All together, these data indicated a good preclinical safety profile of SHR-A1811.

Table 3
GLP toxicology study summary of SHR-A1811 in cynomolgus monkeys

Doses	3 mg/kg	10 mg/kg	40 mg/kg
No. of animal	5/sex/group		
Regimens	Intravenous, every 3 weeks (5 times in total)		
Mortality	No report	No report	No report
Clinical signs	Normal	Normal	Normal
Body weight and food intake	Normal	Normal	Normal
Cardiac function	Normal	Normal	Normal
Hematology	Normal	Normal	Reticulocyte number and percentage decrease by 80%
Clinical chemistry at day2	Normal	Normal	Normal
Target organs and tissue	Normal	Normal	Thymus weight and organ coefficient decrease by 71%
HNSTD	40 mg/kg		

Table 4
Toxicokinetics parameters of SHR-A1811 (40 mg/kg) in cynomolgus monkeys after single and multiple doses

TK Parameters	Payload		Total antibody		SHR-A1811	
	Single	Multiple	Single	Multiple	Single	Multiple
T _{max} (day)	0.269	0.350	0.0569	0.0243	0.0406	0.0243
C _{max} (ng/ml)	1.44	1.48	779038	1046468	649048	801109
AUC _t (day*ng/ml)	5.76	6.34	4232223	5451542	3111089	3988273
AUC _{INF} (day*ng/ml)	6.67	7.14	4904112	6316239	3489237	4524900
t _{1/2} (day)	4.46	4.21	7.53	7.49	6.80	7.06
RacAUC _{INF}	/	1.07	/	1.29	/	1.30

Discussion

The adverse effects of ADCs result from both on-target and off-target toxicities, the latter often caused by systemic release of free toxins and non-specific uptake of antibodies. The mechanisms underlying why T-DXd induced ILD/pneumonitis remain unclear. Considering the adequate blood flow and long retention time in lung, the free payload in circulation may lead to lung damage [25]. There is also a low expression level of HER2 on pulmonary bronchial epithelial cells. Recent studies in monkeys described that target-independent uptake of T-DXd into alveolar macrophages might be another possibility [26]. The success of the 3rd -generation ADC has proven that the bystander killing effect can overcome the challenges such as tumor penetration and antigen heterogeneity, and dramatically improve the clinical benefits in solid tumors [10, 27]. Therefore, to reduce the undesired toxicities of anti-HER2 ADC, our strategy was to increase the membrane permeability of payload while keep topoisomerase I inhibitory activity unchanged. As a result of enhanced bystander killing capability, an ADC carrying less drug load can still be highly efficacious and, most importantly, potentially accompanied with a better safety profile.

To achieve this purpose, SHR169265 was developed via introducing a chiral cyclopropyl at the carbonyl alpha position of exatecan derivative (Fig. 1A). Such structural modification improved liposolubility, membrane permeability and systemic clearance. The inhibitory potency on topoisomerase I was retained (Table 1). The faster clearance could decrease the systemic exposure to free payload and

associated toxicities. The increased membrane permeability eventually led to the stronger cytotoxicity of SHR169265 (Table 2), and improved bystander killing capacity of ADCs. SHR-A1811 with DAR 6 demonstrated a comparable bystander killing potency with HRA18-C015 (T-DXd analog, DAR 8) (Fig. 1B and C), although the *in vitro* cytotoxicity of SHR-A1811 was slightly weaker (Table 2). We rationalized that the enhanced permeability and bystander killing effect of SHR169265 could compensate for the reduced DAR in *in vivo* efficacy study. As expected, SHR-A1811 treatment caused a potent and sustained inhibition of tumor growth in a dose-dependent manner, comparable or even better than HRA18-C015, across HER2 low-to-high expressing xenograft models (Fig. 2). This observation indicated that the stronger bystander killing potency could indeed translate into the *in vivo* antitumor effect of SHR-A1811. The tumoral concentration of payload was proportional to the dosages of ADCs, while circulating toxin was undetectable. Payload accumulation in tumors may contribute to the potent antitumor activity of SHR-A1811. Taken together, SHR-A1811 with DAR 6 showed strong enough antitumor efficacy, presumably attributed to its remarkable bystander killing capacity.

The chemical modification of SHR169265 was anticipated to form a proper steric hindrance and shield when connecting with the linker, and thus enhance the chemical stability of linker-payload system. As expected, high stability in plasma of different species was observed. After 21-day incubation, only less than 1% of payload was released (Fig. 3B). The reported release rate of payload from T-DXd ranged from 1.2–3.9% in mouse, rat, monkey, and human plasma [8]. These stability results were further confirmed by the toxicokinetics study in cynomolgus monkey. Concentrations of SHR-A1811 and total antibody in plasma after multiple doses were similar. The maximum concentration of payload was approximately one part of 500,000 of SHR-A1811 (Fig. 4 and Table 4).

The preclinical toxicology studies of T-DXd in cynomolgus monkeys found that the HNSTD of T-DXd was 30 mg/kg with administration once every 3 weeks for 3 doses. The major target organs were bone marrow, pulmonary, intestine, skin and testis [8]. Consistently, the most common adverse reactions of T-DXd in patients were neutropenia, leukopenia and anemia etc., with ILD/pneumonitis as AE of special interest [12]. In our hands, administration of 40 mg/kg SHR-A1811 in monkeys once every 3 weeks for up to 4 months led to decrease in reticulocyte number and thymus weight, without observations in other organs. The HNSTD of SHR-A1811 in monkeys was determined as 40 mg/kg. The favorable safety profiles possibly could be well explained by the lower drug load, trace amount of free toxin in circulation and high systemic clearance of payload.

In the multi-center, dose-escalation phase I clinical trial (NCT04446260), SHR-A1811 was well tolerated and showed promising antitumor activity in heavily pretreated patients with HER2-expressing or mutant advanced cancers. Patients received intravenous doses of SHR-A1811 ranging from 1 to 8.0 mg/kg every 3 weeks with median duration of follow up at 6.8 months. The ORR in HER2-positive and HER2 low-expressing breast cancer patients were 76.9% and 49.4%, respectively [28]. The ORR in HER2-expressing/mutant non-breast solid tumor patients, including biliary tract cancers, colorectal cancer, gastric cancer, gastroesophageal junction adenocarcinoma and colorectal cancer, was 45.9% [29]. The incidence of all grade ILD was 3.2%. It was worth noting that, of the 103 patients in the 6.4 mg/kg group, only one patient had drug-related ILD. In this dose cohort, the C_{max} and AUC_{inf} of free payload in plasma was 3.7 ng/mL and 24.7 ng.day/mL after multiple dosing [28]. The reported ILD incidence of T-DXd at the same dosage in breast cancer patients was 21% [16] with the C_{max} and AUC_{inf} of free payload at 6.8 ng/mL and 34.2 ng.day/mL [30]. We speculated that the less DAR and low free payload plasma exposure might both contribute to the tolerability of SHR-A1811. More studies will be performed in the future to validate the preliminary clinical findings.

In summary, with a highly permeable payload, optimized DAR, great potency and better safety profiles, SHR-A1811 has demonstrated the best-in-class potential. Currently SHR-A1811 has entered phase II and phase III clinical studies for breast cancer, gastric cancer, colorectal cancer, and NSCLC (NCT05424835, NCT05482568, NCT04818333, NCT05349409).

Abbreviations

HER2: human epidermal growth factor receptor 2

ADC: antibody–drug conjugate

DAR: drug-to-antibody ratio

T-DXd: trastuzumab deruxtecan

NSCLC: non-small cell lung cancer

IHC: immunohistochemistry

FISH: fluorescence in situ hybridization

ILD: interstitial lung disease

GGFG: glycyl-glycyl-phenylalanyl-glycyl

PAMPA: parallel artificial membrane permeability

TGI: tumor growth inhibition

Declarations

Data Availability Statement:

The data generated in this study are available upon request from the corresponding authors.

Conflicts of Interest

Ting Zhang, Jianyan Xu, Junzhao Yin, Yun Gao, Beibei Fu, Jiakang Sun, Zhibing Xu, Shiwei Tu, Yuchang Mao, Weiyun Wen, Bolei Qu, Lingfeng You, Zhendong Xue, Xing Sun, Dan Cao, Jun Feng, Min Hu, and Feng He are employees of Jiangsu HengRui Medicine Co., Ltd. The authors declare no potential conflicts of interest.

Acknowledgements

Not applicable

Fundings

None

Ethics declarations

Ethics approval and consent to participate

Animal experiments at Shanghai Hengrui were approved by the Institutional Animal Care and Use Committee of Shanghai Hengrui (Reference number: 20210317-mouse-1, 20210317-mouse-4, 20210317-mouse-6). Animal studies at Shanghai InnoStar approved by InnoStar's Institutional Animal Care and Use Committee (Reference number: IACUC-2021-M-029). All animal studies were carried out in accordance with ARRIVE guidelines.

Contributions

Ting Zhang designed the experiments, analyzed the data, interpreted the results and wrote the original draft. Min Hu and Feng He supervised this project, interpreted the results and revised the manuscript. Jianyan Xu designed and optimized SHR169265. Junzhao Yin, Yun Gao, Hanwen Zheng, Beibei Fu, Jiakang Sun, Zhibing Xu, Shiwei Tu carried out the *in vitro* and *in vivo* efficacy experiments. Bolei Qu and Lingfeng You were responsible for the compound and ADC synthesis. Yuchang Mao, Zhendong Xue, Weiyun Wen and Xing Sun carried out the pharmacokinetics and toxicity experiments. Dan Cao and Jun Feng were responsible for project management. All authors reviewed the manuscript.

References

1. Yan M, Schwaederle M, Arguello D, Millis SZ, Gatalica Z, Kurzrock R. HER2 expression status in diverse cancers: review of results from 37,992 patients. *Cancer Metastasis Rev.* 2015;34(1):157–64.
2. Yan M, Parker BA, Schwab R, Kurzrock R. HER2 aberrations in cancer: implications for therapy. *Cancer Treat Rev.* 2014;40(6):770–80.
3. Oh DY, Bang YJ. HER2-targeted therapies - a role beyond breast cancer. *Nat reviews Clin Oncol.* 2020;17(1):33–48.
4. Keam SJ. Trastuzumab Deruxtecan: First Approval. *Drugs.* 2020;80(5):501–8.

5. Modi S, Jacot W, Yamashita T, Sohn J, Vidal M, Tokunaga E, Tsurutani J, Ueno NT, Prat A, Chae YS, et al. Trastuzumab Deruxtecan in Previously Treated HER2-Low Advanced Breast Cancer. *N Engl J Med.* 2022;387(1):9–20.
6. Shitara K, Bang YJ, Iwasa S, Sugimoto N, Ryu MH, Sakai D, Chung HC, Kawakami H, Yabusaki H, Lee J, et al. Trastuzumab Deruxtecan in Previously Treated HER2-Positive Gastric Cancer. *N Engl J Med.* 2020;382(25):2419–30.
7. Li BT, Smit EF, Goto Y, Nakagawa K, Udagawa H, Mazieres J, Nagasaka M, Bazhenova L, Saltos AN, Felip E, et al. Trastuzumab Deruxtecan in HER2-Mutant Non-Small-Cell Lung Cancer. *N Engl J Med.* 2022;386(3):241–51.
8. Ogitani Y, Aida T, Hagihara K, Yamaguchi J, Ishii C, Harada N, Soma M, Okamoto H, Oitate M, Arakawa S, et al. DS-8201a, A Novel HER2-Targeting ADC with a Novel DNA Topoisomerase I Inhibitor, Demonstrates a Promising Antitumor Efficacy with Differentiation from T-DM1. *Clin cancer research: official J Am Association Cancer Res.* 2016;22(20):5097–108.
9. Yver A, Agatsuma T, Soria JC. The art of innovation: clinical development of trastuzumab deruxtecan and redefining how antibody-drug conjugates target HER2-positive cancers. *Annals of oncology: official journal of the European Society for Medical Oncology.* 2020;31(3):430–4.
10. Ogitani Y, Hagihara K, Oitate M, Naito H, Agatsuma T. Bystander killing effect of DS-8201a, a novel anti-human epidermal growth factor receptor 2 antibody-drug conjugate, in tumors with human epidermal growth factor receptor 2 heterogeneity. *Cancer Sci.* 2016;107(7):1039–46.
11. Narayan P, Osgood CL, Singh H, Chiu HJ, Ricks TK, Chiu Yuen Chow E, Qiu J, Song P, Yu J, Namuswe F, et al. FDA Approval Summary: Fam-Trastuzumab Deruxtecan-Nxki for the Treatment of Unresectable or Metastatic HER2-Positive Breast Cancer. *Clin cancer research: official J Am Association Cancer Res.* 2021;27(16):4478–85.
12. Rugo HS, Bianchini G, Cortes J, Henning JW, Untch M. Optimizing treatment management of trastuzumab deruxtecan in clinical practice of breast cancer. *ESMO open.* 2022;7(4):100553.
13. Tarantino P, Modi S, Tolaney SM, Cortes J, Hamilton EP, Kim SB, Toi M, Andre F, Curigliano G. Interstitial Lung Disease Induced by Anti-ERBB2 Antibody-Drug Conjugates: A Review. *JAMA Oncol.* 2021;7(12):1873–81.
14. DaiichiSankyo I. atfda_docs/label/2019/76113_9s000_lbl.pdf. Accessed : Enhertu (fam-trastuzumab deruxtecan-nxki): US prescribing information. In. <https://www.accessdata.fda.gov/drugs> 2022; 2022.
15. Abuhelwa Z, Alloghbi A, Alqahtani A, Nagasaka M. Trastuzumab Deruxtecan-Induced Interstitial Lung Disease/Pneumonitis in ERBB2-Positive Advanced Solid Malignancies: A Systematic Review. *Drugs.* 2022;82(9):979–87.
16. Tamura K, Tsurutani J, Takahashi S, Iwata H, Krop IE, Redfern C, Sagara Y, Doi T, Park H, Murthy RK, et al. Trastuzumab deruxtecan (DS-8201a) in patients with advanced HER2-positive breast cancer previously treated with trastuzumab emtansine: a dose-expansion, phase 1 study. *Lancet Oncol.* 2019;20(6):816–26.
17. Modi S, Saura C, Yamashita T, Park YH, Kim SB, Tamura K, Andre F, Iwata H, Ito Y, Tsurutani J, et al. Trastuzumab Deruxtecan in Previously Treated HER2-Positive Breast Cancer. *N Engl J Med.* 2020;382(7):610–21.
18. Cortes J, Kim SB, Chung WP, Im SA, Park YH, Hegg R, Kim MH, Tseng LM, Petry V, Chung CF, et al. Trastuzumab Deruxtecan versus Trastuzumab Emtansine for Breast Cancer. *N Engl J Med.* 2022;386(12):1143–54.
19. Carter P, Presta L, Gorman CM, Ridgway JB, Henner D, Wong WL, Rowland AM, Kotts C, Carver ME, Shepard HM. Humanization of an anti-p185HER2 antibody for human cancer therapy. *Proc Natl Acad Sci U S A.* 1992;89(10):4285–9.
20. Lewis Phillips GD, Li G, Dugger DL, Crocker LM, Parsons KL, Mai E, Blättler WA, Lambert JM, Chari RVJ, Lutz RJ, et al. Targeting HER2-Positive Breast Cancer with Trastuzumab-DM1, an Antibody–Cytotoxic Drug Conjugate. *Cancer Res.* 2008;68(22):9280–90.
21. Xu J, Zhang Y, Cai XF, Qu B, Liang J, Zhang L, He F, Tao W. Ligand-drug conjugate of exatecan analogue, preparation method therefor and application thereof. In. Edited by WIPO. International; 2020.
22. Lyon RP, Meyer DL, Setter JR, Senter PD. Conjugation of anticancer drugs through endogenous monoclonal antibody cysteine residues. *Methods Enzymol.* 2012;502:123–38.
23. Lombardo F, Shalaeva MY, Tupper KA, Gao F, Abraham MH. ElogPoct: a tool for lipophilicity determination in drug discovery. *J Med Chem.* 2000;43(15):2922–8.
24. He N, Yang CP, Yang Y, Xue ZD, Xu JY, Sun X, Yang CY, Feng J, Ye X, Zhang Z et al. SHR-A1921, a novel TROP-2 ADC with an optimized design and well balanced profile between efficacy and safety. *American Association for Cancer Research Annual Meeting 2023*, Abstract nr LB030.
25. Fu Z, Li S, Han S, Shi C, Zhang Y. Antibody drug conjugate: the biological missile for targeted cancer therapy. *Signal Transduct Target therapy.* 2022;7(1):93.

26. Kumagai K, Aida T, Tsuchiya Y, Kishino Y, Kai K, Mori K. Interstitial pneumonitis related to trastuzumab deruxtecan, a human epidermal growth factor receptor 2-targeting Ab-drug conjugate, in monkeys. *Cancer Sci.* 2020;111(12):4636–45.
27. Ocana A, Amir E, Pandiella A. HER2 heterogeneity and resistance to anti-HER2 antibody-drug conjugates. *Breast cancer research: BCR.* 2020;22(1):15.
28. Yao H, Yan M, Tong Z, Wu X, Ryu M, Kim JH, Zhong JP, Han Y, Liu W. C : Safety, tolerability, pharmacokinetics, and antitumor activity of SHR-A1811 in HER2-expressing/mutated advanced solid tumors: A global phase 1, multi-center, first-in-human study [abstract CT175]. *Cancer Res* 2023, 83(8_Supplement).
29. Yao HRMH, Park J, Voskoboynik M, Kim JH, Liu K, Barve M, Acuna-Villaorduna A, Im S-A, Roy AC, Bai L-Y, Yen C-J, Zhang J, Ganju V, Wu L, Yan M, Bao L, Zhao Y, Rong S, Song E. The HER2-targeting ADC SHR-A1811 in HER2-expressing/mutated advanced non-breast solid tumors (STs): Results from the global phase I study [abstract 656MO]. *Annals of Oncology* 2023, 34, supplement 2(52):S461-S462.
30. Doi T, Shitara K, Naito Y, Shimomura A, Fujiwara Y, Yonemori K, Shimizu C, Shimoi T, Kuboki Y, Matsubara N, et al. Safety, pharmacokinetics, and antitumour activity of trastuzumab deruxtecan (DS-8201), a HER2-targeting antibody-drug conjugate, in patients with advanced breast and gastric or gastro-oesophageal tumours: a phase 1 dose-escalation study. *Lancet Oncol.* 2017;18(11):1512–22.

Figures

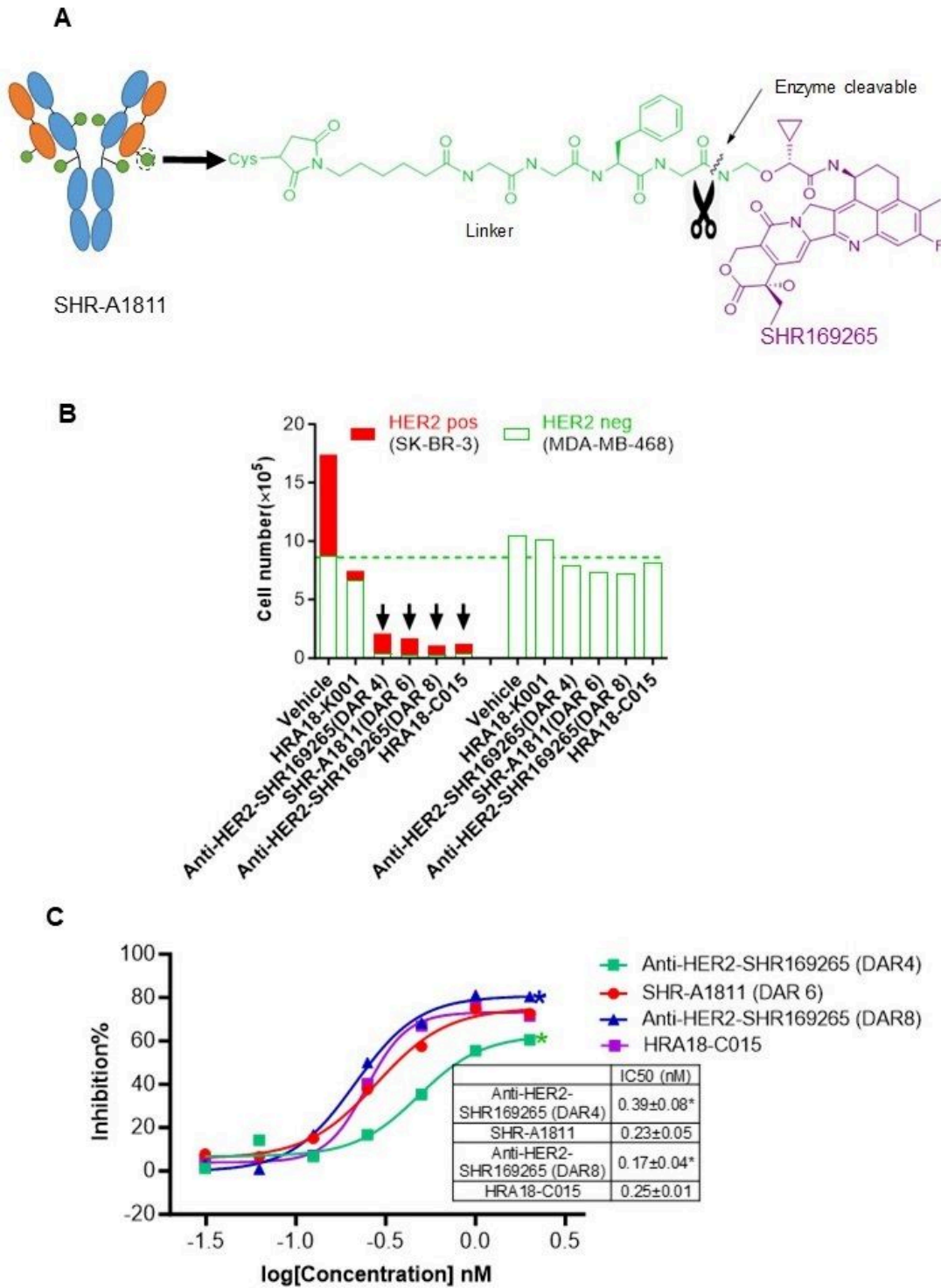


Figure 1

Structure and bystander killing effect of anti-HER2-SHR169265 ADCs. **A**, Structure illustration of SHR-A1811. SHR-A1811 is composed of trastuzumab, a stable and cleavable linker, and a topoisomerase I inhibitor payload SHR169265, with DAR at 6. **B**, Bystander killing effect of anti-HER2-SHR169265 ADCs. SK-BR-3 (HER2-positive) and MDA-MB-468 (HER2-negative) cells were co-cultured and treated. For comparison, MDA-MB-468 cells were cultured alone and treated in the same way. Cell numbers of SK-BR-3 and MDA-MB-468 cells after treatment with 10 nM of ADCs for 5 days were analyzed. **C**, The inhibitory effect of ADCs on MDA-MB-468 in the co-culture system for bystander killing. Cells were treated with various doses of ADCs for 3 days. Data represented three independent experiments. * $P < 0.05$ versus HRA18-C015.

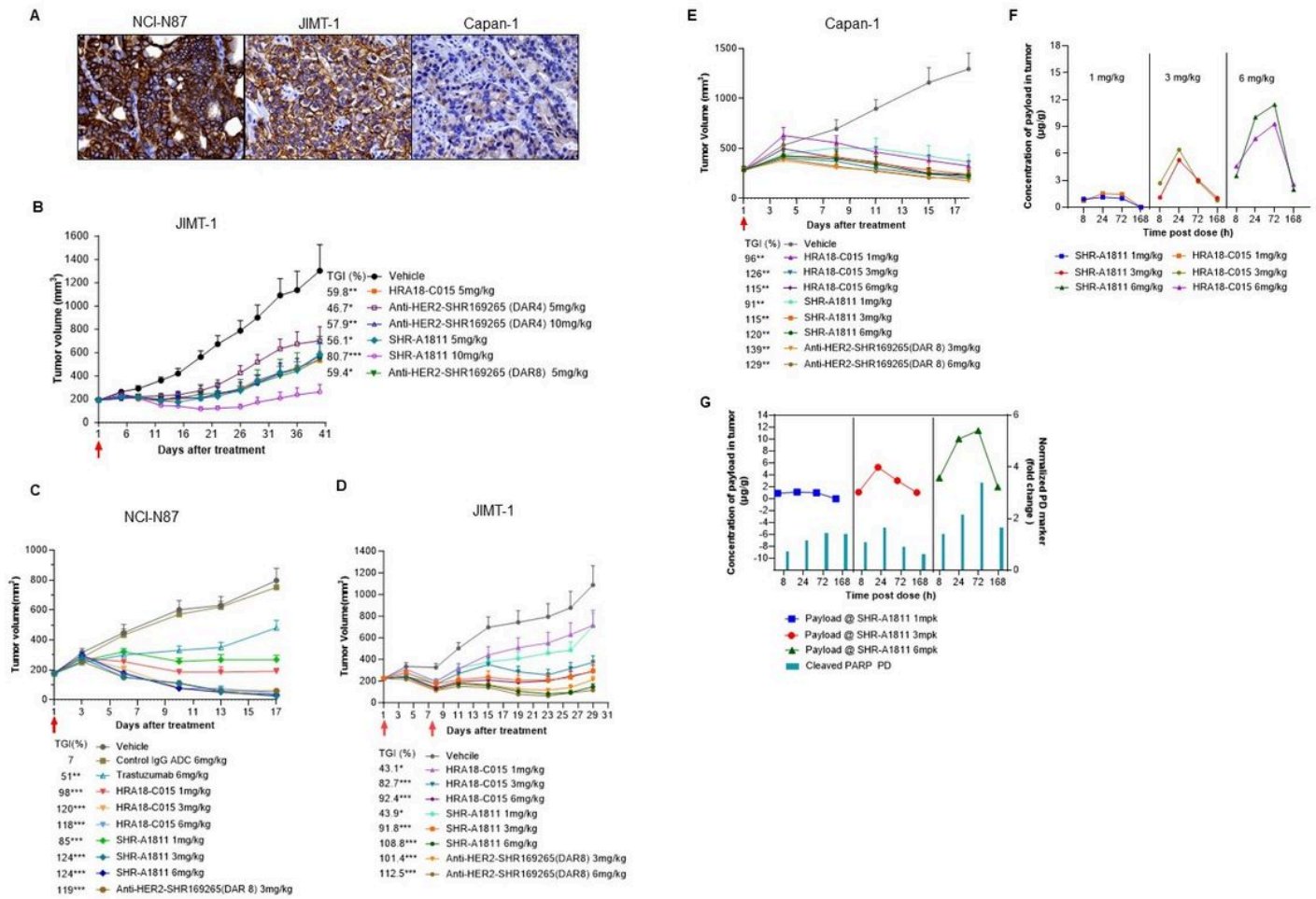
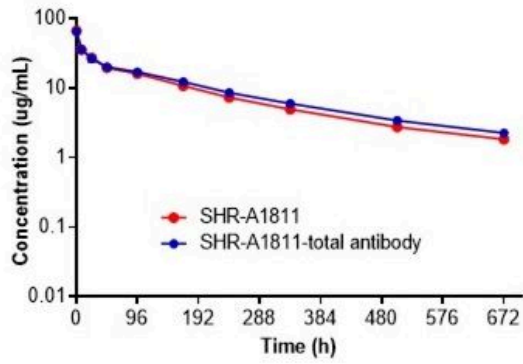
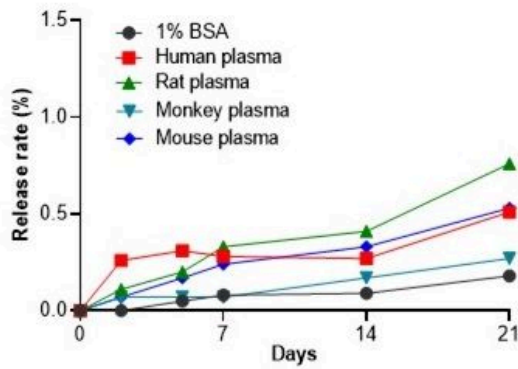


Figure 2

Antitumor effect of anti-HER2-SHR169265 ADCs.

A, HER2 IHC staining on NCI-N87, JIMT-1 and Capan-1 xenografted tumors. **B**, Comparison of antitumor effect of anti-HER2-SHR169265 ADCs with different DAR values in JIMT-1 xenograft model. **C-E**, Antitumor effect of SHR-A1811 in NCI-N87 (**C**), JIMT-1 (**D**) and Capan-1 (**E**) xenograft models. The tumor-bearing mice were intraperitoneally administered with ADCs single dose or every week for two weeks. Arrows indicate days of administration. The mean tumor volume and SEM (n = 6-8) were represented on the graph, and TGI% calculated for each treatment group. *P<0.05, **P<0.01, ***P<0.001 versus vehicle. **F**, The concentration of SHR-169265 and SHR-167971 in NCI-N87 tumors after single dose of SHAR-A1811 and HRA18-C015. **G**, PK/PD relationship of SHR-A1811 in NCI-N87 model. The tumoral SHR169265 concentration and cleaved PARP level were measured at 8, 24, 72 and 168 hours after single dose of ADC. Data shown as means from two tumor samples.

A**B****Figure 3**

Pharmacokinetics and plasma stability of SHR-A1811. **A**, Pharmacokinetics of SHR-A1811 in rats. SHR-A1811 were intravenously administered at the dose of 3 mg/kg (n=3). Concentrations of SHR-A1811 and total antibody were measured. **B**, *In vitro* stability of SHR-A1811 in plasma of different species. SHR-A1811 was incubated in mouse, rat, monkey, and human plasma at 37°C for up to 21 days. The concentrations of released payload were detected, and release rates (%) was calculated.

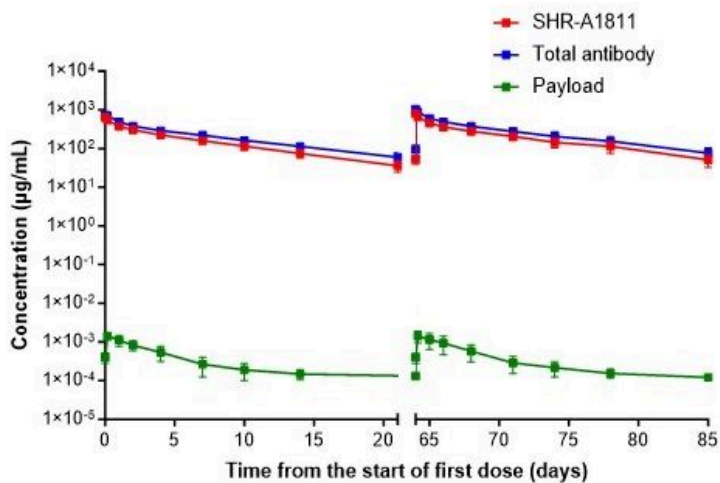


Figure 4

Toxicokinetics of SHR-A1811 in cynomolgus monkeys. SHR-A1811 was intravenously administered at the dose of 40 mg/kg every 3 weeks for 5 doses (n=10). SHR-A1811, total antibody and payload concentrations were measured after the first and fourth doses. Data shown as means from ten samples.

Supplementary Files

This is a list of supplementary files associated with this preprint. Click to download.

- [SupplementaryData202310.pptx](#)